


|  |   |
|--|---|
|  <b>MLF Experimental Report</b>   | 提出日 Date of Report<br>Oct 31, 2013  |
| 課題番号 Project No.<br>2013A0178<br>実験課題名 Title of experiment<br>Development of neutron scintillation detectors<br>実験責任者名 Name of principal investigator<br>Masaki Katagiri<br>所属 Affiliation<br>Ibaraki University, Frontier Research Center for Applied Atomic Sciences | 装置責任者 Name of responsible person<br>Dr. Oikawa<br>装置名 Name of Instrument/(BL No.)<br>NOBORU /(BL10)<br>実施日 Date of Experiment<br>Apr 26-28, 2013, May 17-18, 2013 |

試料、実験方法、利用の結果得られた主なデータ、考察、結論等を、記述して下さい。(適宜、図表添付のこと)  
 Please report your samples, experimental method and results, discussion and conclusions. Please add figures and tables for better explanation.

1. 試料 Name of sample(s) and chemical formula, or compositions including physical form.  
 No sample was used in the experiment. The detector performances were purely evaluated using a collimated pulsed neutron beam only.

2. 実験方法及び結果 (実験がうまくいかなかった場合、その理由を記述してください。)  
 Experimental method and results. If you failed to conduct experiment as planned, please describe reasons.

In this allocated experimental time the detector performances of (i) ZnS/<sup>6</sup>LiF neutron scintillator, and (ii) New type of fibre-optic-taper detector were evaluated.

**(i) Neutron scintillator materials**

We have developed new neutron scintillators for several kinds of neutron detectors for iBIX detector, Senju detector, Takumi detector, PSPMT detector, FOT detector, monitor detector and neutron imaging detector (CCD camera). The scintillators for these detectors are necessary to optimize the performance by changing the mixing ratio of ZnS/neutron converter, thickness and binder condition for TOF experiments depending on the neutron energy range of interest. The basic neutron detection and optical properties of the scintillator were evaluated as a function of time-of-flight.

New-type ZnS/<sup>6</sup>LiF scintillators with several kinds of binders were developed for high detection efficiency and high counting rate. Figure 1 shows typical structure of a developed ZnS/<sup>6</sup>LiF scintillator with a binder. Mixing ratio of ZnS and <sup>6</sup>LiF was 1.5:1 and several kind of binders were evaluated as a function of time-of-flight.

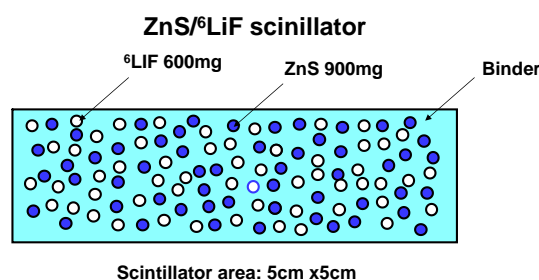
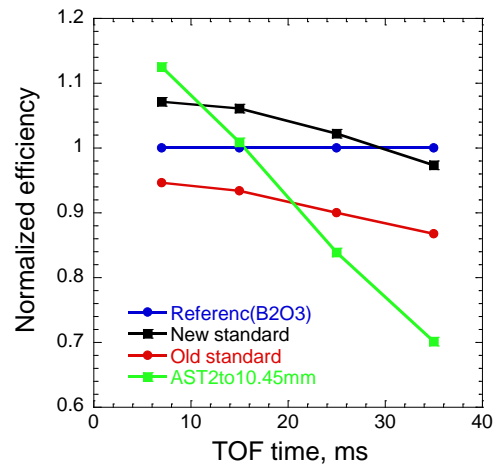


Figure 1 Typical structure of a developed ZnS/<sup>6</sup>LiF scintillator with a binder

## 2. 実験方法及び結果(つづき) Experimental method and results (continued)

In the experiments, the scintillator was attached on the front of crossed WLS fiber bundles of iBIX detector and evaluated. Figure 2 shows comparison results of AST2to1 scintillator (world standard), J-PARC new standard (organic binder) and J-PARC old standard (inorganic binder) that are used for RPMT detectors and neutron radiography when a  $^{10}\text{B}_2\text{O}_3$  scintillator used for a new iBIX detector is employed as the reference scintillator. The TOF characteristics of the scintillators were measured at the distance of 12.5 m from the mercury target. The  $\lambda(\text{\AA})$  is obtained by  $\text{TOF}(\mu\text{s})/3160$ . It is confirmed that the efficiency of AST2to1 scintillator decreases rapidly according to increase of the TOF time and the efficiency of J-PARC new standard scintillator is improved with 15% to that of the old standard in full range of TOF time.



### (ii) New detector development for neutron TOF imaging

New detector for neutron TOF imaging was developed and its detector performances were evaluated. Figure 3 shows a photograph of the neutron-detecting head of the detector and the side view. The scintillation image generated in the scintillator with a thickness of 100  $\mu\text{m}$  was magnified by two-stages of the fibre-optic-taper device to a magnification ratio of 9.6. The effective pixel size of the detector becomes 52  $\mu\text{m}$ . Beam edge was measured with the prototype detector at the BL10. Figure 4 shows beam profiles (a) without a FOT and (b) with the FOTs. The FWHM spatial resolution was further improved by inserting the FOT devices, from 1.36

mm to 0.156 mm. It was also demonstrated in the lab that the detector had a low gamma-ray sensitivity of  $10^{-6}$ .

mm to 0.156 mm. It was also demonstrated in the lab that the detector had a low gamma-ray sensitivity of  $10^{-6}$ .

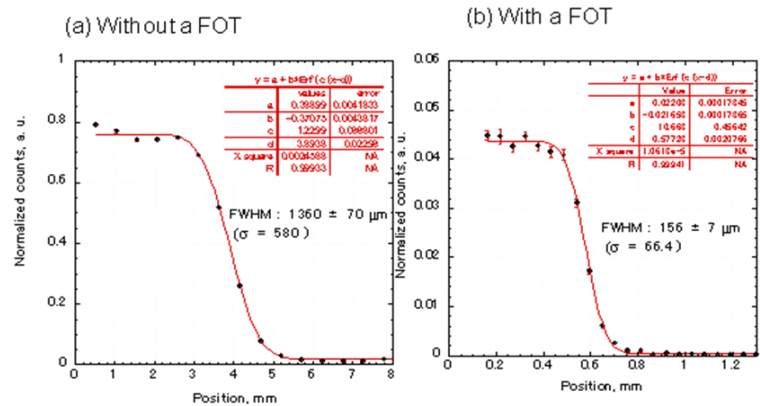


Figure 4 Beam edge profiles fitted by edge spreading function

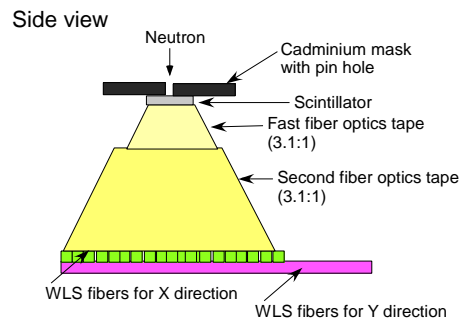
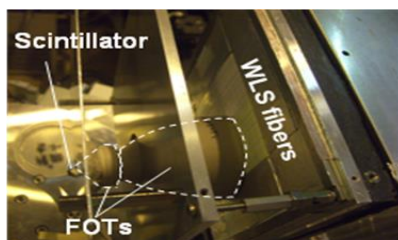


Figure 3 Photograph of a FOT detector and side view